Journal of Chemical Ecology (2018) 44:497–509
https://doi.org/10.1007/s10886-018-0945-1

Acylated Quinic Acids Are the Main Salicortin Metabolites in the Lepidopteran Specialist Herbivore *Cerura vinula*

Felix Feistel[1] · Christian Paetz[1] · Riya C. Menezes[1] · Daniel Veit[1] · Bernd Schneider[1]

Received: 22 December 2017 / Revised: 4 March 2018 / Accepted: 8 March 2018 / Published online: 17 March 2018

Abstract

Salicortin is a phenolic glucoside produced in Salicaceae as a chemical defense against herbivory. The specialist lepidopteran herbivorous larvae of *Cerura vinula* are able to overcome this defense. We examined the main frass constituents of *C. vinula* fed on *Populus nigra leaves*, and identified 11 quinic acid derivatives with benzoate and/or salicylate substitution. We asked whether the compounds are a result of salicortin breakdown and sought answers by carrying out feeding experiments with highly ^{13}C-enriched salicortin. Using HRMS and NMR analyses, we were able to confirm that salicortin metabolism in *C. vinula* proceeds through deglucosylation and ester hydrolysis, after which saligenin is oxidatively transformed into salicylic acid and, eventually, conjugated to quinic acid. To the best of our knowledge, this is the first report of a detoxification pathway based on conjugation with quinic acid.

Keywords *Cerura vinula* · *Populus nigra* · Salicortin · Down-stream metabolism · Salicaceae · Stable isotope labeling

Introduction

Salicinoids – glycosides derived from salicyl alcohol (saligenin) – are defensive chemicals of *Populus* species and of other members of the Salicaceae family (Lindroth 1991; Palo 1984). The structural diversity of salicinoids arises from their modular composition, which comprises a saligenin core unit, a glucose moiety and an organic acid. The most representative salicinoid in *Populus* is salicortin (**12**), as so far it has been found in all investigated species (Boeckler et al. 2011; Thieme 1964). Numerous studies have investigated the effect of salicinoids on lepidopteran herbivorous insects, such as *Papilio glaucus* (Lindroth 1991), *Choristoneura conflictica* (Clausen et al. 1989), *Malacosoma disstria* and *Lymantria dispar* (Lindroth and Hemming 1990) or *Operophtera brumata* (Boeckler et al. 2016; Ruuhola et al. 2001). Coleopteran larvae belonging to the Chrysomelidae family can sequester salicinoids and use their host plant's chemical defense to ward off predators (Burse et al. 2009). Recently, a comprehensive study of the generalist herbivore *L. dispar* (Boeckler et al. 2016) provided the first detailed description of how a lepidopteran detoxifies salicinoid compounds. The digestive degradation of salicinoids in the insect gut (Haruta et al. 2001; Lindroth 1988; Ruuhola et al. 2003) results in saligenin and an *o*-quinone (Clausen et al. 1989; Julkunen-Tiitto and Meier 1992; Knuth et al. 2011). Both metabolites are known for their toxic and feeding-deterrent activities (Boeckler et al. 2011; Clausen et al. 1989; Ruuhola et al. 2001).

The larva of the lepidopteran *Cerura vinula* is native to Europe and Asia. In the temperate climate zone of Central Europe, imagines appear from April to August. Females lay eggs on branches and leaves of their host plants. As the insects' nutritional spectrum is limited to plants of the Salicaceae family (*Salix* and *Populus* species), they are regarded as specialist herbivores (Ali and Agrawal 2012; Hintze-Podufal 1970). Numerous metabolic studies (recent examples: Beran et al. 2014; Joussen et al. 2012; Shelomi et al. 2016) have addressed the question whether a specialist herbivore uses a distinct mechanism to cope with the defense of its host plant. In the present publication, we used a double-track strategy: the careful structural identification of metabolic products arising from the diet of the specialist herbivore resulted in an assumption about how the main chemical defense compounds were transformed during digestion. This hypothesis was then supported using stable isotope labeling which eventually allowed us to develop a new salicinoid degradation pathway.

Electronic supplementary material The online version of this article (https://doi.org/10.1007/s10886-018-0945-1) contains supplementary material, which is available to authorized users.

✉ Bernd Schneider
schneider@ice.mpg.de

[1] Max Planck Institute for Chemical Ecology, Hans-Knöll-Straße 8, Beutenberg Campus, D-07745 Jena, Germany

Methods and Materials

General Information In order to address the question of how *C. vinula* is able to deactivate the salicinoid defense of its host plant, several experimental approaches were employed. It was necessary to develop UPLC-MS and NMR protocols for the identification of the main metabolites as well as an HPLC-SPE protocol for the degradation-free workup of the compounds of interest. [^{13}C]-Labeling of salicinoids was accomplished *in planta* by growing plants under a [^{13}C]CO_2-enriched atmosphere in a dedicated growth chamber and subsequent isolation of [U-^{13}C]salicortin from leaf material. Experimental details and procedures can be found in the following section.

NMR spectra for the structure elucidation of acylated quinic acids **1** to **11** were recorded on a Bruker Avance III HD 700 MHz spectrometer, equipped with a 1.7 mm TCI microcryoprobe (Bruker Biospin, Rheinstetten, Germany) using NMR tubes of 1.7 mm outer diameter. NMR spectra of frass extracts from *C. vinula* larvae after [U-^{13}C]salicortin feeding experiments were obtained on a Bruker Avance III HD 500 MHz NMR spectrometer equipped with a 5 mm TCI cryoprobe (Bruker Biospin) using NMR tubes of 5 mm outer diameter. NMR spectra for the characterization of *in vivo*-generated [U-^{13}C]salicortin were recorded on a Bruker Avance III HD 400 MHz NMR spectrometer equipped with a 5 mm BBFO probe (Bruker Biospin) using NMR tubes of 5 mm outer diameter. NMR spectra were recorded using MeOH-d_4 as a solvent. Chemical shifts were referenced to the residual solvent peaks at δ_H 3.31 and δ_C 49.15. Data acquisition and processing were accomplished using TopSpin 3.2. Standard pulse programs as implemented in TopSpin were used for data acquisition.

The ultra-high-performance liquid chromatography–electrospray ionization–tandem mass spectrometry system (UHPLC–ESI–MS/MS) for structure elucidation and analysis of frass compounds after [U-^{13}C]salicortin labeling consisted of an Ultimate 3000 series RSLC (Dionex, Sunnyvale, CA, USA) and a Q Exactive Plus - Orbitrap mass spectrometer (Thermo Fisher Scientific, Bremen, Germany) using heated-electrospray ionization (H-ESI). H-ESI source parameters were set to 4 kV for spray voltage and 35 V for transfer capillary voltage at a capillary temperature of 300 °C. The samples were measured in positive and negative ionization mode in the mass range of *m/z* 100 to 1000 using 70,000 $m/\Delta m$ resolving power in the Orbitrap mass analyzer.

UHPLC-ESI-MS/MS for hemolymph analysis was performed with an Ultimate 3000 series RSLC (Dionex) and LTQ - Orbitrap XL mass spectrometer (Thermo Fisher Scientific) in which ionization was accomplished using electrospray ionization (ESI). ESI source parameters were set to 4 kV for spray voltage, 35 V for transfer capillary voltage at a capillary temperature 275 °C. The samples were measured in negative ionization mode in the mass range of *m/z* 100 to 1000 using 30,000 m/Δm resolving power in the Orbitrap mass analyzer. All UHPLC systems used an Acclaim C18 column (150 × 2.1 mm, 2.2 μm, Dionex, Sunnyvale, CA, USA) for chromatographic separation. HRMS data were evaluated and interpreted using Xcalibur software (Thermo Fisher Scientific, Waltham, MA, USA).

HPLC-ESI-MS of acylated quinic acids **1**–**11** was performed on an Agilent 1100 HPLC system, consisting of a degasser, quaternary solvent delivery pump G1311A, an autosampler G1313A (Agilent Technologies, Waldbronn, Germany), a photodiode array detector (detection 200–700 nm; J&M Analytik, Aalen, Germany) and an Esquire 3000 ion trap mass spectrometer (Bruker Daltonik, Bremen, Germany). The column outlet was connected to a Bruker/Spark Holland Prospect 2 solid-phase extraction (SPE) system (Bruker Biospin) for post-column SPE trapping on HySphere resin GP cartridges. To reduce the eluotropic capacity of the HPLC solvent mixture, water was added with a flow rate of 2.5 ml min^{-1} using a make-up pump (Knauer, Berlin, Germany).

[U-^{13}C]Salicortin was chromatographically purified on an Agilent 1100 HPLC system, consisting of a degasser G1322A, a binary pump G1312A, an autosampler G1313A and a photodiode array detector G1315B (Agilent Technologies). The column outlet was connected to an Advantec CHF122SB fraction collector (Jasco, Gross-Umstadt, Germany) triggered by a relay board from the Agilent 1100. HPLC separations were carried out using an Isis RP-18e column (250 × 4.6 mm, 5 μm particle size) (Macherey-Nagel, Düren, Germany). Solvents were evaporated with a rotary evaporator Rotavapor R-114 (Büchi Labortechnik, Flawil, Switzerland) and a Genevac HT-4X vacuum centrifuge (Genevac, Ipswich, UK). Homogenization was carried out with a MINILYS cell disruptor (Bertin Technologies, Montigny-le-Bretonneux, France). Solvents used for extraction and chromatographic separation were purchased from Carl Roth (Karlsruhe, Germany) and VWR International (Darmstadt, Germany), and used without further purification. Acetonitrile and water (hypergrade for LCMS) used for UHPLC-ESI-MS/MS were purchased from Merck (Darmstadt, Germany), and formic acid (eluent additive for LC-MS) was obtained from Sigma Aldrich (Steinheim, Germany). Water used for HPLC was obtained from a Milli-Q Synthesis A 10 purifier (Merck). $^{13}CO_2$ (isotopic purity 99 atom% ^{13}C, <3 atom% ^{18}O) and Phytacon™ vessels (H 140 mm, base diam. 86 mm) used as arenas for the larvae feeding experiments were purchased from Sigma-Aldrich (Taufkirchen, Germany). HR-X SPE cartridges (500 mg sorbent/6 ml volume), folded filters (90 mm) and paper filters (MN 615 ¼, 125 mm) were purchased from Macherey-Nagel. Syringe filters (0.45 μm, PA) were purchased from Carl Roth. (−)-Quinic acid was purchased from Thermo Fisher Kandel (Karlsruhe, Germany).

Plant Material and Insect Larvae Plant samples of black poplar (*P. nigra*) were collected from trees growing in proximity to the Max Planck Institute for Chemical Ecology in Jena, Germany. *P. nigra* is a typical hostplant of *C. vinula* (Hintze-Podufal 1970) in natural habitats and was therefore used to raise the larvae for the experiments. *P. trichocarpa x deltoides* Beaupré were grown in the greenhouse of the Max Planck Institute for Chemical Ecology. The species was thoroughly examined in previous studies regarding its spectrum of salicinoid defense compounds (Feistel et al. 2015). The light period was set from 6:30 to 20:30 (14 h), while temperatures were kept between 21 and 23 °C during the day and between 19 and 21 °C at night. The humidity was regulated between 50 to 60%. Puss moth (*C. vinula*) larvae were hatched from eggs and reared on *P. nigra* leaves in the laboratory.

Extraction and Isolation of *C. vinula* Frass. Frass of *C. vinula* larvae fed on *P. nigra* leaves were collected and lyophilized, resulting in 73 g of dry material. Contaminated material (leaves, petioles and exuviae) was removed manually. Dried frass (20 g) were ground using a ceramic mortar and pestle, and extracted (5 × 200 ml, each 10 min) with MeOH. The extracts were filtered (paper filters and 0.45 μm PA syringe filters), pooled and evaporated under reduced pressure, resulting in 2.5 g dried crude extract. This dry matter (53.8 mg) was suspended in water (20 ml) using ultrasound and subjected to pre-separation on a HR-X SPE (PS/DVB) cartridge. After conditioning with MeOH (2 × 6 ml) and equilibration with water (3 × 6 ml), the cartridge was loaded with the extract suspension and washed with water (3 × 6 ml). After drying in vacuum, the cartridge was eluted with MeOH (3 × 6 ml). The eluate was then dried using a vacuum centrifuge, resulting in 24.7 mg pre-purified extract. For separation, an aliquot dissolved in MeOH (67.4 mg ml^{-1}) was subjected to HPLC-SPE. A binary solvent system of 0.1% formic acid in water (solvent A) and 0.1% formic acid in MeOH (solvent B) was used for HPLC separation, starting with a 5 min isocratic flow of 100% solvent A and decreasing linearly for 90 min to 50% solvent A. Column temperature was set to 35 °C and the solvent flow rate was 0.8 mL min^{-1}. After each run, the column was washed with 100% MeOH for 5 min and equilibrated with 100% H_2O for 10 min. SPE cartridges loaded with metabolites were dried in a stream of N_2 gas before being eluted with MeOH. Eluted compounds were dried by vacuum centrifugation, yielding the following compounds (R_t retention time): **1** (R_t 32.69 min, 2.1 mg g^{-1} dry frass), **4** (R_t 36.69 min, 1.2 mg g^{-1}), **5** (R_t 39.71 min, 1.1 mg g^{-1}), **2** (R_t 41.00 min, 2.6 mg g^{-1}), **3** (R_t 52.59 min, 3.4 mg g^{-1}), **10** (R_t 61.70 min, 1.6 mg g^{-1}), **7** (R_t 64.14 min, 2.1 mg g^{-1}), **9** (R_t 65.52 min, 3.0 mg g^{-1}), **6** (R_t 68.34 min, 2.8 mg g^{-1}), **11** (R_t 70.18 min, 2.1 mg g^{-1}), **8** (R_t 72.73 min, 1.9 mg g^{-1}).

Structure elucidation was carried out using 1D (^{1}H NMR, selective TOCSY) and 2D NMR (^{1}H-^{1}H COSY, ^{1}H-^{13}C HSQC, ^{1}H-^{13}C HMBC) spectra recorded at 700 MHz and UHPLC-ESI-MS/MS measurements (Q Exactive Plus - Orbitrap MS) using a binary solvent system of H_2O (solvent A) and acetonitrile (solvent B), both of which contained 0.1% (*v*/v) formic acid with a flow rate of 300 μl min^{-1}. The linear gradient used started with 0% B and increased to 100% B within 15 min. Afterwards, the column was washed for 5 min with 100% B and then equilibrated at 0% B for 5 min.

***In Vivo* Generation and Isolation of ^{13}C-Labeled Salicortin** Stable isotope labeling was achieved in a growth chamber resembling a setup described previously (Chen et al. 2011). The greenhouse light system (Philips SON-T Agro 400 W) was used to provide constant light exposure from 6:30 to 22:00 (15.5 h). Temperature and relative humidity were kept between 20 °C to 30 °C and 50% to 80%, respectively. Six *P. trichocarpa x deltoides* Beaupré plants were pruned to a height of about 30 cm, leaving a few basal leaves. After being transferred to the growth chamber, plants were kept in darkness for the first 2 days. At the beginning of day 3, the respired CO_2 (natural abundance isotope ratio) was removed from the chamber's atmosphere and 450 ppm $^{13}CO_2$ was injected into it. This $^{13}CO_2$ level was kept constant during the entire experimental time (26 days). At the end of each day's light period, $^{13}CO_2$ injection was stopped and respired CO_2 was continuously removed during the night. Details about the $^{13}CO_2$ labeling are provided in the supporting information (B.1 and B.2).

The $^{13}CO_2$-labeling experiment was stopped at day 28, and newly grown plant tissue (leaves with petioles) was collected and lyophilized yielding 13 g dry material. The material was manually crushed and filled equally into Falcon tubes (8 × 45 ml) containing steel beads (3 mm). Extraction was accomplished with MeOH (30 ml per tube) in a Skandex S-7 paint shaker (Fluid Management, Wheeling, IL, USA) for 2 × 4 min. Afterwards, the extracts were pooled, filtered, and the solvent was evaporated in vacuo, yielding 4.18 g (32% dw) dry matter. The dry matter was suspended in 500 ml H_2O, divided into 3 parts and subjected to solid-phase extraction on HR-X SPE columns (each 1.5 g sorbent). After loading, columns were washed with H_2O (3 × 20 ml) and eluted with MeOH (20 ml). The combined methanolic fractions were dried in vacuo, yielding 2.26 g pre-purified extract (17.33% dw). An aliquot solution (121 mg ml^{-1}) was subjected to HPLC separation.

[U-^{13}C]Salicortin was separated using a binary solvent system consisting of 0.1% formic acid in H_2O (solvent A) and 0.1% formic acid in MeOH (solvent B). Column temperature was set to 35 °C and the solvent flow rate was 0.8 ml min^{-1}. The HPLC gradient that was used started with a 5 min isocratic flow of 100% solvent A and decreased linearly for 5 min to 85%, 25 min to 70% and finally 50 min to 50% solvent A. Afterwards, the column was washed for 10 min

with 100% MeOH and equilibrated for 10 min with 100% H_2O. The salicortin UV signal peak (λ = 285 nm) appeared at R_t 42.6 min. Unlabeled salicortin (natural abundance ^{13}C) was isolated in the same manner from unlabeled *P. trichocarpa x deltoides* tissue.

Characterization of the salicortin isolated from the ^{13}C-labeled plant tissue and calculation of its ^{13}C-enrichment was done by means of ^{1}H, ^{13}C and ^{1}H-^{13}C HSQC NMR spectra (400 MHz) and HPLC-ESI-MS measurements using the chromatographic method as described above. The *in vivo*-generated salicortin showed uniform ^{13}C-labeling with 82% total ^{13}C-enrichment. Spectroscopic data of the [U-^{13}C]salicortin (82% ^{13}C) and detailed information about the calculation of the ^{13}C-enrichment are presented in the Supplementary data (SI B.2).

[U-^{13}C]Salicortin Larval Feeding Freshly cut leaves of *P. nigra* (LPI 3–10) were used for feeding experiments. The leaf petioles were inserted into 2 ml Eppendorf micro reaction vessels. Lids of the vessels were removed for convenient handling prior to being filled with tap water. The opening of the vessels was sealed with Parafilm® fastening the leaf petioles to prevent the water in the vessel from spilling. An aqueous solution of [U-^{13}C]salicortin (2.5 mg ml^{-1}) was spotted evenly on the surface of 5 poplar leaves (10 × 20 µl droplets per leaf). Control leaves were spotted with water in an analogous fashion. Leaves were left under the fume hood for 3 h, allowing the droplets to dry completely. Subsequently, the [U-^{13}C]salicortin-coated leaves and the control leaves were transferred into arenas for feeding experiments. Each arena contained one leaf and one *C. vinula* larva (late 3rd to early 4th instars), which were placed onto the surface of each leaf. The larvae were kept in the arena until the leaves had been completely consumed. Frass collected from the control experiments and the stable isotope feeding experiments, respectively, were pooled into 2 batches which were subsequently lyophilized.

The freeze-dried frass was then extracted with MeOH (3 × 1 ml) by homogenization in a Minilys cell disruptor (2 ml tubes, 60 s and 4000 rpm), using 1.4 mm o.d. ZrO_2 beads. The supernatants from each sample were pooled and evaporated using N_2 gas and subsequently extracted with H_2O (5 × 1 ml). The aqueous extracts were pooled and dried with N_2 gas. Afterwards, methanolic and aqueous extracts of frass from control and [U-^{13}C]salicortin feeding experiments were subjected to NMR (500 MHz) and UHPLC-ESI-MS/MS (Q Exactive Plus – Orbitrap MS) analysis, using the chromatographic system described above.

Collection of *C. vinula* Hemolymph The question of whether salicinoid metabolites are detectable in the hemolymph of *C. vinula* larvae was addressed as follows: 6 *C. vinula* larvae (3 × control, 3 × fed with [U-^{13}C]salicortin) were immobilized in 15 ml Falcon tubes and kept in the −20 °C freezer for 15 min. A mid-abdominal proleg of an anesthetized larva was pierced with a scalpel, and the emerging hemolymph was transferred by means of a pipette into an ice-cooled 2 ml Eppendorf micro reaction vessel containing MeOH (1 ml). Subsequently, the mixture was centrifuged and the supernatant was evaporated by a stream of N_2 gas, yielding an average amount of 3.07 mg (SD ± 1.51 mg) residue per larva. Each of the 6 dried residues were dissolved in 1 ml MeOH and analyzed independently by UHPLC-ESI-MS/MS (LTQ - Orbitrap XL MS), using a binary solvent system of H_2O (solvent A) and acetonitrile (solvent B), both of which contained 0.1% (*v*/v) formic acid with a flow rate of 300 µl min^{-1}. A linear gradient was used, starting with 5% B to 52% B within 20 min. Afterwards, the column was washed for 5 min with 100% B and then equilibrated at 5% B for another 5 min.

Results

***C. vinula* Frass Analysis** Frass of *C. vinula* larvae fed on *P. nigra* leaves was collected and metabolites extracted as described in the Methods and Materials section. Eleven quinic acid derivatives representing almost 2.5% (23.9 mg g^{-1}) of the frass dry mass were identified (Fig. 1). Among them, 10 compounds (**1**–**3, 5**–**11**) were unknown and only compound **4** had been reported recently (Wan et al. 2016). For an overview about NMR, HR-MS and UV data, see Tables 1, 2, 3 and 4. Spectra of all compounds, including salicortin (**12**) and quinic acid (**13**), are provided in the Supplementary data (SI A.1 to A.13).

The HRESIMS data of compound **1** showed a molecular ion peak at *m/z* 311.0774 $[M\text{-}H]^-$ corresponding to a molecular formula of $C_{14}H_{16}O_8$ (calcd for $C_{14}H_{15}O_8$, *m/z* 311.0772). The ^{1}H NMR spectrum of compound **1** (Table 1) showed signals of 11 protons assignable to 2 different structural units. In the low-field region of the ^{1}H NMR spectra, we observed signals of an asymmetric 4-spin system (ABCD) at δ_H 6.62 ($^{3}J_{HH}$ = 0.8/8.3 Hz; H-3′), δ_H 7.21 ($^{3}J_{HH}$ = 1.5/7.3/8.3 Hz; H-4′), δ_H 6.60 ($^{3}J_{HH}$ = 0.8/6.9/7.3 Hz; H-5′) and δ_H 7.44 ($^{3}J_{HH}$ = 1.4/6.9 Hz; H-6′), characteristic of a 1,2-disubstituted aromatic ring. The corresponding ^{13}C chemical shifts were determined by an ^{1}H-^{13}C hetero-correlation single quantum coherence (HSQC) spectrum as δ_C 118.8 (C-3′), δ_C 135.5 (C-4′), δ_C 119.5 (C-5′) and δ_C 132.5 (C-6′). Further evidence for a 1,2-disubstitution was provided by an ^{1}H-^{13}C heteronuclear multiple-bond correlation (HMBC) spectrum showing $^{3}J_{CH}$ correlations from H-4′ and H-6′ to a quaternary carbon atom at δ_C 159.9 (C-2′) as well as from H-3′ and H-5′ to another quaternary carbon atom at δ_C 115.2 (C-1′). Because of its low-field ^{13}C chemical shift, C-2′ was assigned as oxygenated. Furthermore, H-6′ (δ_H 7.44) showed a long-range CH-correlation to a carboxyl functionality at δ_C 167.7 (C-7′)

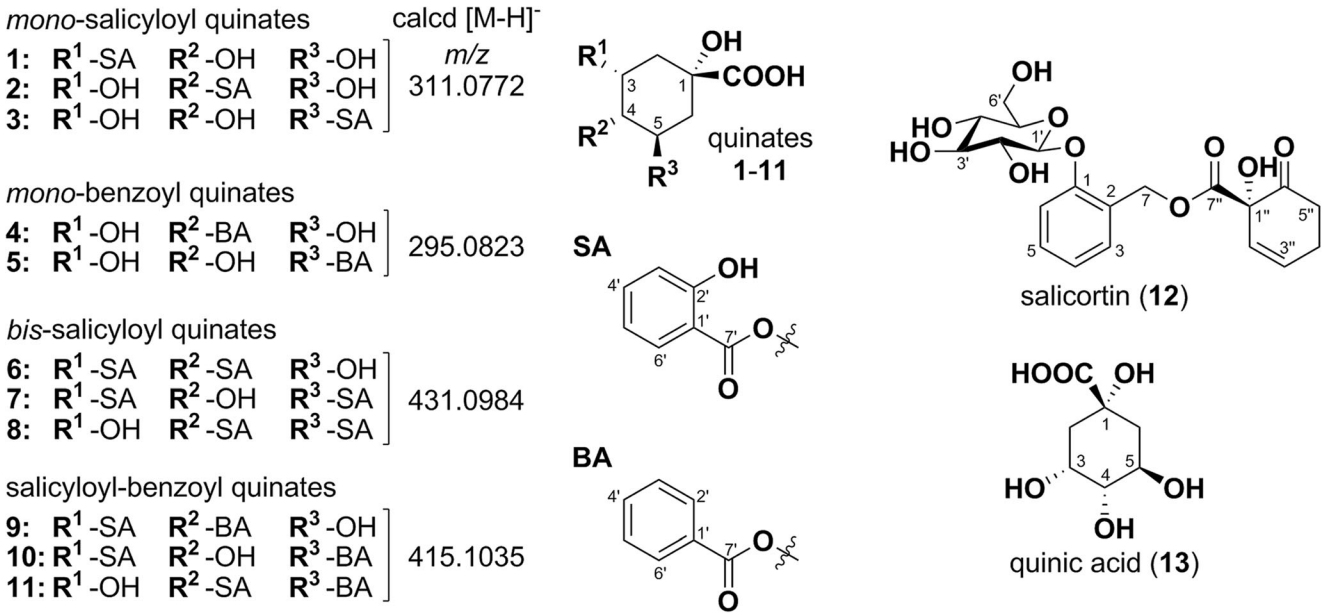

Fig. 1 Metabolites isolated from frass of *C. vinula* larvae fed on *P. nigra* leaves, and the structures of salicortin (**12**) and quinic acid. SA: salicyloyl; BA: benzoyl

tethered to C-1′ (δ_C 115.2). Thus, the data suggest the presence of a salicyloyl moiety (SA). A double-doublet signal of a methine appeared at δ_H 5.70 ($^3J_{HH}$ = 3.1/3.4/3.1; H-3). The corresponding ^{13}C chemical shift was extracted from the ^1H-^{13}C HSQC spectrum at δ_C 72.8 (C-3), which is characteristic for a hydroxylated aliphatic carbon atom. Adjacent to H-3, another methine at δ_H 3.60 ($^3J_{HH}$ = 3.4/9.5 Hz; H-4), and a methylene group at δ_H 2.35 ($^3J_{HH}$ = 3.1/14.4 Hz; H-2a) and δ_H 2.11 ($^3J_{HH}$ = 3.1/14.4 Hz; H-2b) were determined from their $^3J_{HH}$ correlations by ^1H-^1H COSY. Furthermore, consecutive cross-peaks from H-4 to another methine at δ_H 4.06 ($^3J_{HH}$ = 4.6/9.5/12.0 Hz; H-5) and to a second methylene group at δ_H 2.10 ($^3J_{HH}$ = 12.0/12.5 Hz; H-6a) and δ_H 1.95 ($^3J_{HH}$ = 4.6/12.5 Hz; H-2b) were observed. The small $^3J_{HH}$ values (3.4 Hz) for H-3 and H-4 indicated equatorial configuration, whereas the large values (9.5 Hz) for H-4 and H-5 indicated axial configuration. The corresponding ^{13}C-chemical shifts were determined by ^1H-^{13}C

Table 1 ^1H NMR (700 MHz) and ^{13}C NMR (175 MHz) data of compounds **1–4** in MeOH-d_4

Position	**1**		**2**		**3**		**4**	
	δ_H mult. (*J* in Hz)	δ_C	δ_H mult. (*J* in Hz)	δ_C	δ_H mult. (*J* in Hz)	δ_C	δ_H mult. (*J* in Hz)	δ_C
1		80.3		76.4		76.2		76.5
2a	2.35 *dd* (3.1/14.4)	36.8	2.12 *dd* (2.8/14.5)	38.3	2.22 *dd* (2.3/14.1)	38.6	2.19 *dd* (2.6/13.6)	39.1
2b	2.11 *dd* (3.1/14.4)		2.07 *ddd* (2.6/3.8/14.5)		2.06 *dd* (4.4/14.1)		2.06 *dd* (2.7/13.6)	
3	5.70 *ddd* (3.1/3.4/3.1)	72.8	4.35 *ddd* (2.8/2.9/3.8)	69.5	4.19 *ddd* (2.3/3.2/4.4)	71.3	4.37 *ddd* (2.2/2.6/2.7)	68.7
4	3.60 *dd* (3.4/9.5)	75.6	5.02 *dd* (2.9/9.4)	80.0	3.83 *dd* (3.2/8.4)	72.9	5.02 *dd* (2.2/7.8)	79.1
5	4.06 *ddd* (4.6/9.5/12.0)	68.0	4.39 *ddd* (4.7/9.4/10.8)	65.6	5.55 *ddd* (3.6/8.4/9.6)	73.3	4.29 *ddd* (5.4/7.8/9.8)	66.3
6a	2.10 *dd* (12.0/12.5)	42.5	2.20 *ddd* (2.6/4.7/13.3)	42.0	2.28 *dd* (3.6/13.1)	38.6	2.15 *dd* (5.4/14.5)	39.1
6b	1.77 *dd* (4.6/12.5)		1.89 *dd* (10.8/13.3)		2.21 *dd* (9.6/13.1)		2.05 *dd* (9.8/14.5)	
7		182.6		181.8		177.5		179.8
1’		115.2		113.8		113.5		131.5
2’		159.9		162.6		162.7	8.13 *dd* (0.9/8.0)	130.6
3’	6.62 *dd* (0.8/8.3)	118.8	6.95 *d* (8.5)	118.0	6.94 *dd* (0.8/8.4)	118.0	7.49 *dd* (8.0/7.6)	129.2
4’	7.21 *ddd* (1.5/7.3/8.3)	135.5	7.49 *ddd* (1.6/7.4/8.5)	136.8	7.48 *ddd* (1.3/7.2/8.4)	136.6	7.61 *dd* (7.6/7.6)	134.0
5’	6.60 *ddd* (0.8/6.9/7.3)	119.5	6.93 *dd* (7.4/7.4)	120.0	6.91 *ddd* (0.8/7.2/8.0)	120.1	7.49 *dd* (8.0/7.6)	129.2
6’	7.44 *dd* (1.4/6.9)	132.5	8.05 *dd* (1.6/7.4)	131.6	7.88 *dd* (1.3/8.0)	131.1	8.13 *dd* (0.9/8.0)	130.6
7’		167.7		170.8		170.7		167.7

Table 2 ^{1}H NMR (700 MHz) and ^{13}C NMR (175 MHz) data of compounds **5–8** in MeOH-d_4

Position	**5**		**6**		**7**		**8**	
	δ_H mult. (*J* in Hz)	δ_C	δ_H mult. (*J* in Hz)	δ_C	δ_H mult. (*J* in Hz)	δ_C	δ_H mult. (*J* in Hz)	δ_C
1		77.3		75.0		79.9		77.3
2a	2.19 *dd* (3.9/13.8)	38.8	2.24 *dd* (2.8/15.1)	42.2	2.26 *dd* (3.2/14.8)	36.6	2.14 *m*	38.4
2b	1.98 *dd* (2.9/13.8)		2.48 *dd* (3.2/15.1)		2.41 *dd* (3.4/14.8)		2.38 *m*	
3	4.15 *ddd* (2.6/2.9/3.9)	72.9	5.95 *ddd* (2.8/3.2/3.4)	70.9	5.71 *ddd* (3.2/3.4/3.4)	74.2	4.49 *ddd* (2.9/3.2/3.6)	69.6
4	3.97 *dd* (2.6/9.4)	74.8	5.28 *dd* (3.4/9.2)	77.3	4.13 *dd* (3.4/8.9)	71.7	5.42 *dd* (2.9/9.4)	76.9
5	5.52 *ddd* (4.9/9.4/11.1)	73.3	4.48 *ddd* (6.6/9.2/10.9)	65.6	5.71 *ddd* (4.8/8.9/11.7)	73.3	5.95 *ddd* (6.7/8.3/9.4)	70.3
6a	2.19 *dd* (11.1/14.9)	40.1	2.13 *dd* (10.9/13.7)	42.2	2.30 *dd* (11.7/12.8)	39.9	2.37 *m*	39.4
6b	2.11 *dd* (4.9/14.9)		2.31 *dd* (6.6/13.7)		2.33 *dd* (4.8/12.8)		2.37 *m*	
7		176.2		177.5		182.3		178.8
1’		131.6		133.8		113.9		113.0
2’	8.06 *dd* (1.2/8.3)	130.5		161.9		162.1		162.1
3’	7.47 *dd* (7.4/8.3)	129.4	6.92 *d* (8.5)	118.5	6.94 *d* (8.5)	118.2	6.88 *d* (8.5)	118.1
4’	7.59 *dd* (7.4/7.4)	134.1	7.48 *ddd* (1.5/7.3/8.5)	136.7	7.47 *ddd* (1.2/6.9/8.5)	136.3	7.42 *ddd* (1.2/8.2/8.5)	137.1
5’	7.47 *dd* (7.4/8.3)	129.4	6.90 *dd* (7.3/7.9)	120.2	6.94 *dd* (6.9/8.0)	120.1	6.85 *dd* (8.0/8.2)	120.4
6’	8.06 *dd* (1.2/8.3)	130.5	7.91 *dd* (1.5/7.9)	131.8	8.04 *dd* (1.2/8.0)	132.2	7.88 *dd* (1.2/8.0)	131.1
7’		168.1		169.3		169.8		170.5
1”				113.4		113.9		113.0
2”				162.4		162.9		162.4
3”			6.93 *d* (8.5)	118.0	6.93 *d* (8.3)	118.1	6.87 *d* (8.5)	118.1
4”			7.44 *ddd* (1.5/7.1/8.5)	136.7	7.49 *ddd* (1.5/6.9/8.3)	136.7	7.43 *ddd* (1.3/7.8/8.5)	137.1
5”			6.74 *dd* (7.1/7.9)	120.0	6.93 *dd* (6.9/8.1)	120.1	6.83 *dd* (7.8/7.8)	120.4
6”			7.62 *dd* (1.5/7.9)	130.9	7.92 *dd* (1.5/8.1)	131.0	7.75 *dd* (1.3/7.8)	130.7
7”				170.6		170.3		170.4

HSQC as δ_C 36.8 (C-2), δ_C 75.6 (C-4), δ_C 68.0 (C-5) and δ_C 42.5 (C-6). As for C-3 (δ_C 72.8), large ^{13}C NMR chemical shift values indicated oxygenation for C-4 and C-5. The ^{1}H-^{13}C HMBC spectrum revealed a $^{3}J_{CH}$ correlation of H-3 with an oxygenated quaternary carbon atom at δ_C 80.3 (C-1). Furthermore, both methylene groups (H-2ab and H-6ab) showed weak long-range CH correlations to C-1, as a result of which the entire aliphatic structure can be characterized as a cyclohexane ring system. Another HMBC correlation from H-6b to a quaternary carbon at δ_C 182.6 (C-7) tethered to C-1 revealed quinic acid. The characteristic low-field shift of H-3 indicated substitution in this position. This assumption was further supported by an ^{1}H-^{13}C HMBC correlation from H-3 to the carboxyl carbon C-7′ (δ_C 167.7) of the salicyloyl moiety. Accordingly, the structure of compound **1** was assigned as 3-*O*-salicyloyl quinic acid.

Similar to **1**, the HRESIMS spectra of compounds **2** and **3** showed a molecular ion peak of *m/z* 311.0773 [M-H]$^-$, again corresponding to a molecular formula of $C_{14}H_{16}O_8$ (calcd for $C_{14}H_{15}O_8$, *m/z* 311.0772). The data from ^{1}H NMR, ^{1}H-^{1}H COSY, ^{1}H-^{13}C HSQC and the ^{1}H-^{13}C HMBC spectra resembled those of compound **1** (Table 1). Signals of the salicyloyl moiety and the quinic acid subunit were present, but the substitution patterns differed at C-3, C-4 and C-5 of the quinic acid moieties. Acylation of the hydroxyl groups in (−)-quinic acid (**13**) leads to low-field shifts of the signals of H-3, H-4 and H-5 (Pauli et al. 1998). However, the multiplicities and coupling constants remain unaffected. Thus, the shift of a characteristic multiplet to the low field indicates the substitution site (Fig. 2). The multiplets of H-4 (δ_H 5.02) in the ^{1}H NMR spectrum of compound **2** and H-5 (δ_H 5.55) in the spectrum of compound **3** – which in comparison with the corresponding signals of quinic acid (**13**) appeared at the low field – revealed esterification with salicyloyl units at the hydroxyl groups in positions 4 and 5, respectively.

The structures of **2** and **3** were further characterized by ^{1}H-^{13}C HMBC correlations of H-4 (**2**; δ_H 5.02) and H-5 (**3**; δ_H 5.55) with the carboxylic carbon atoms of their salicyloyl moieties at δ_C 170.8 (**2**; C-7′) and 170.7 (**3**; C-7′), respectively. Accordingly, compound **2** was identified as 4-*O*-salicyloyl quinic acid and compound **3** was identified as 5-*O*-salicyloyl quinic acid.

The analytical data of compound **4** were in accordance with previously reported 4-*O*-benzoyl quinic acid (Wan et al. 2016). The HRESIMS spectra of compound **5** showed a molecular ion peak of *m/z* 295.0819 [M-H]$^-$, corresponding to a

Table 3 ^{1}H NMR (700 MHz) and ^{13}C NMR (175 MHz) data of compounds **9–11** in MeOH-d_4

Position	**9**		**10**		**11**	
	δ_H mult. (*J* in Hz)	δ_C	δ_H mult. (*J* in Hz)	δ_C	δ_H mult. (*J* in Hz)	δ_C
1		75.2		75.1		72.9
2a	2.22 *dd* (3.7/14.8)	37.2	2.26 *dd* (5.3/14.8)	36.6	2.11 *dd* (3.7/14.7)	38.7
2b	2.47 *dd* (3.2/14.8)		2.40 *dd* (4.6/14.8)		2.38 *dd* (3.6/14.7)	
3	5.93 *ddd* (3.2/3.3/3.7)	71.0	5.71 *ddd* (2.9/4.9/5.3)	74.4	4.47 *ddd* (3.1/3.6/3.7)	70.0
4	5.22 *dd* (3.3/9.2)	77.0	4.12 *dd* (2.9/8.3)	71.8	5.41 *dd* (3.1/9.5)	77.6
5	4.46 *ddd* (3.7/9.2/9.2)	65.8	5.56 *ddd* (5.6/8.3/10.0)	72.9	5.91 *ddd* (4.2/9.5/11.2)	69.8
6a	2.12 *dd* (9.2/14.4)	42.0	2.29 *dd* (10.0/13.5)	39.2	2.36 *m*	40.0
6b	2.30 *dd* (3.7/14.4)		2.29 *dd* (5.6/13.5)		2.36 *m*	
7		178.5		177.6		178.3
1’		113.8		114.1		113.2
2’		161.9		162.0		162.9
3’	6.92 *dd* (0.7/8.5)	118.3	6.93 *d* (8.2)	118.3	6.87 *dd* (0.5/8.7)	118.1
4’	7.48 *ddd* (1.1/7.5/8.5)	136.6	7.47 *dd* (7.4/8.2)	136.5	7.42 *ddd* (1.9/7.5/8.7)	136.8
5’	6.90 *ddd* (0.7/7.5/7.9)	120.1	6.94 *dd* (7.4/7.5)	120.0	6.83 *ddd* (0.5/7.5/7.9)	120.1
6’	7.88 *dd* (1.1/7.9)	131.8	8.04 *d* (7.5)	132.1	7.88 *dd* (1.9/7.9)	131.2
7’		169.5		169.7		170.9
1”		131.1		131.0		131.2
2”	7.91 *dd* (1.1/8.2)	130.4	8.06 *d* (8.5)	130.5	7.92 *dd* (1.0/8.1)	130.3
3”	7.39 *dd* (7.5/8.2)	129.2	7.49 *dd* (7.4/8.5)	129.2	7.40 *dd* (7.6/8.1)	129.3
4”	7.57 *dd* (7.5/7.5)	134.1	7.61 *dd* (7.4/7.4)	134.1	7.54 *dd* (7.6/7.6)	134.2
5”	7.39 *dd* (7.5/8.2)	129.2	7.49 *dd* (7.4/8.5)	129.2	7.40 *dd* (7.6/8.1)	129.3
6”	7.91 *dd* (1.1/8.2)	130.4	8.06 *d* (8.5)	130.5	7.92 *dd* (1.0/8.1)	130.3
7”		167.2		167.1		167.0

molecular formula of $C_{14}H_{16}O_7$ (calcd for $C_{14}H_{15}O_7$, *m/z* 295.0823) and indicating an isomer of compound **4**. In accordance with this suggestion, the ^{1}H NMR, ^{1}H-^{1}H COSY, ^{1}H-^{13}C HSQC and the ^{1}H-^{13}C HMBC spectra of compound **5** (Table 2) showed very similar signals in comparison to compound **4**. Thus, both compounds are constitutional isomers consisting of a quinic acid moiety substituted with a benzoyl moiety. Accordingly, the ^{1}H NMR data of compound

Table 4 UV and HRESIMS data of compounds **9–11**

Compound		**UV (MeOH/H_2O)**	**HRESIMS**	
	No. **Calcd for, *m/z* [M-H]$^-$**	**Name**	**λ_{max} (nm)**	***m/z* [M-H]$^-$**
1	3-*O*-Salicyloyl quinic acid	203.5, 237.5, 303.9	311.0774	$C_{14}H_{15}O_8$, 311.0772
2	4-*O*-Salicyloyl quinic acid	203.5, 237.5, 303.9	311.0773	$C_{14}H_{15}O_8$, 311.0772
3	5-*O*-Salicyloyl quinic acid	203.5, 237.0, 305.9	311.0773	$C_{14}H_{15}O_8$, 311.0772
4	4-*O*-Benzoyl quinic acid*	279.4	295.0820	$C_{14}H_{15}O_7$, 295.0823
5	5-*O*-Benzoyl quinic acid	276.4	295.0819	$C_{14}H_{15}O_7$, 295.0823
6	3-*O*,4-*O*-Disalicyloyl quinic acid	204.5, 235.0, 305.4	431.0986	$C_{21}H_{19}O_{10}$, 431.0984
7	3-*O*,5-*O*-Disalicyloyl quinic acid	204.0, 236.0, 304.9	431.0985	$C_{21}H_{19}O_{10}$, 431.0984
8	4-*O*,5-*O*-Disalicyloyl quinic acid	208.0, 306.9	431.0987	$C_{21}H_{19}O_{10}$, 431.0984
9	3-*O*-Salicyloyl-4-*O*-benzoyl quinic acid	302.4	415.1038	$C_{21}H_{19}O_9$, 415.1035
10	3-*O*-Salicyloyl-5-*O*-benzoyl quinic acid	210.0, 309.9	415.1038	$C_{21}H_{19}O_9$, 415.1035
11	4-*O*-Salicyloyl-5-*O*-benzoyl quinic acid	217.5, 283.4	415.1038	$C_{21}H_{19}O_9$, 415.1035

*Reported by Wan et al. 2016

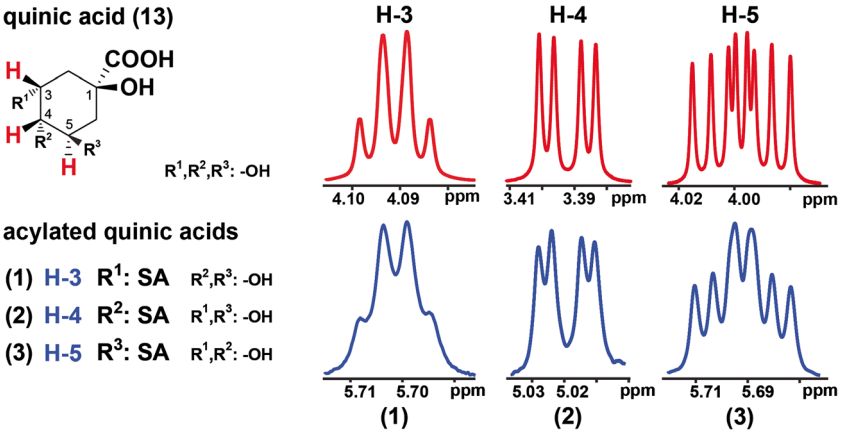

Fig. 2 ^{1}H NMR signals illustrating identical multiplicities and coupling constants of H-3, H-4 and H-5 of (−)-quinic acid (**13**) (red) compared to the corresponding ^{1}H NMR signals of acylated compounds **1**–**3** (blue), shifted to the low field. Full spectra are given in the Supplementary data.

5 showed signals assignable to a symmetrical 5-spin system (AA'XX'Y) at δ_H 8.06 ($^3J_{HH}$ = 1.2/8.3 Hz, H-2′/6′), δ_H 7.47 ($^3J_{HH}$ = 7.4/8.3 Hz, H-3′/5′) and δ_H 7.59 ($^3J_{HH}$ = 7.4/7.4 Hz, H-4′); these signals are characteristic of a mono-substituted aromatic ring. Corresponding ^{13}C chemicals shifts were extracted from the ^{1}H-^{13}C HSQC spectrum at δ_C 130.5 (C-2′/6′), δ_C 129.4 (C-3′/5′) and δ_C 134.1 (C-4′). The aromatic ring structure was further determined by $^3J_{CH}$ correlations in the ^{1}H-^{13}C HMBC spectrum from H-3′/5′ (δ_H 7.47) to a quaternary carbon atom at δ_C 131.6 (C-1′). Another long-range CH-correlation of H-2′/6′ (δ_H 8.06) to a carboxyl carbon atom at δ_C 168.1 (C-7′) tethered to the C-1′ position of the aromatic ring was observed in the HMBC spectrum, confirming the benzoyl moiety. Substitution to the quinic acid moiety was determined by the characteristic low-field shift of the signal of H-5 (δ_H 5.52), indicating substitution at the hydroxyl group at position 5 (δ_C 73.3; δ_H 5.52). Accordingly, the structure of compound **5** was assigned as 5-*O*-benzoyl quinic acid.

The HRESIMS data of compound **6** showed a molecular ion peak of *m/z* 431.0986 [M-H]$^-$, corresponding to a molecular formula of $C_{21}H_{20}O_{10}$ (calcd for $C_{21}H_{19}O_{10}$, *m/z* 431.0984). The ^{1}H NMR, ^{1}H-^{1}H COSY, ^{1}H-^{13}C HSQC and the ^{1}H-^{13}C HMBC spectra of compound **6** (Table 2) showed signals of a quinic acid as well as 2 salicyloyl moieties. The ^{1}H NMR spectra showed characteristic low-field shifts for H-3 (δ_H 5.95) and H-4 (δ_H 5.28), suggesting a bis-substituted quinate. Due to overlapping signals, selective TOCSY together with ^{1}H-^{1}H COSY and ^{1}H-^{13}C HSQC were employed to extract the chemical shifts of both salicyloyl moieties. Connectivities between quinate and salicyloyl moieties were established by ^{1}H-^{13}C long-range correlations of H-3 to δ_C 169.3 (C-7′) and of H-4 to δ_C 170.6 (C-7″), both characterized as carboxyl carbons of the respective salicyloyl units. Accordingly, the structure of compound **6** was assigned as 3-*O*,4-*O*-disalicyloyl quinic acid.

The HRESIMS spectra of compounds **7** and **8** showed molecular ion peaks of *m/z* 431.0985 [M-H]$^-$ and 431.0987 [M-H]$^-$, respectively. As in compound **6**, both values corresponded to a molecular formula of $C_{21}H_{20}O_{10}$ (calcd for $C_{21}H_{19}O_{10}$, *m/z* 431.0984). ^{1}H NMR, ^{1}H-^{1}H COSY, ^{1}H-^{13}C HSQC and the ^{1}H-^{13}C HMBC spectra showed almost the same signals (Table 2), indicating quinic acid esters with salicyloyl moieties as substituents. The structures were characterized by ^{1}H-^{13}C long-range correlations as well as the characteristic chemical shifts of ^{1}H NMR signals for H-3, H-4 and H-5. For compound **7**, we observed low-field shifts for H-3 (δ_H 5.708) and H-5 (δ_H 5.712), suggesting acylation at this positions. The assumption was proven by $^3J_{CH}$ correlations of H-3 to δ_C 169.8 (C-7′) and of H-5 to δ_C 170.3 (C-7″), indicating C-7′ and C-7″ as carboxyl carbons of 2 different salicyloyl moieties. Likewise, for compound **8**, we observed low-field shifts for H-4 at δ_H 5.42, which further showed a $^3J_{CH}$ correlation to δ_C 170.5 (C-7′). The ^{1}H NMR signal of H-5 appeared at δ_H 5.95 with a $^3J_{CH}$ correlation to δ_C 170.4 (C-7″). Accordingly, the structures of the compounds **7** and **8** were assigned as 3-*O*,5-*O*-disalicyloyl quinic acid and 4-*O*,5-*O*-disalicyloyl quinic acid, respectively.

The HRESIMS spectra of compound **9** showed a molecular ion peak of *m/z* 415.1038 [M-H]$^-$ corresponding to a molecular formula of $C_{21}H_{20}O_9$ (calcd for $C_{21}H_{19}O_9$, *m/z* 415.1035). The NMR data (Table 3) extracted from the ^{1}H NMR, ^{1}H-^{1}H COSY, ^{1}H-^{13}C HSQC and the ^{1}H-^{13}C HMBC spectra were very similar to those of compounds **1** and **6**. Accordingly, the presence of a salicyloyl quinate unit was suggested. Furthermore, signals of a benzoyl moiety as described for compound **4** were observed as a substituent of quinic acid. The ^{1}H NMR spectra showed characteristic low-field shifts for H-3 (δ_H 5.93) and H-4 (δ_H 5.22), suggesting substitution at those positions. Cross-signals observed in the ^{1}H-^{13}C HMBC between H-3 and the carboxylic carbon atom C-7′ (δ_C 169.5) of the salicyloyl moiety proved the substitution in position C-3 of the quinic acid via an ester bond. An additional $^3J_{CH}$ correlation of H-4 to the carboxylic carbon atom C-7″ (δ_C 167.2) of the benzoyl moiety revealed another esterification. Accordingly, the structure of compound **9** was assigned as 3-*O*-salicyloyl-4-*O*-benzoyl quinic acid.

Like the data for compound **9**, the HRESIMS data for compounds **10** and **11** showed a molecular ion peak of 415.1038 $[M-H]^-$ corresponding to a molecular formula of $C_{21}H_{20}O_9$ (calcd for $C_{21}H_{19}O_9$, *m/z* 415.1035). The NMR data for both compounds (Table 3) were very similar to those of **9**, suggesting acylated quinic acid derivatives with mixed salicyloyl and benzoyl substituents. The structures of compounds **10** and **11** were elucidated by characteristic ^{1}H NMR chemical shifts and ^{1}H-^{13}C long-range correlations as described for compounds **6**–**8**. For compound **10**, substitution with a salicyloyl group in position 3 (δ_C 74.4; δ_H 5.71) and with the benzoyl unit in position 5 (δ_C 72.9; δ_H 5.56) of the quinic acid was observed. For compound **11**, salicyloyl substitution was observed at position 4 (δ_C 77.6; δ_H 5.41), and benzoylation was found at position 5 (δ_C 69.8; δ_H 5.91) of the quinic acid moiety. Accordingly, the structures were assigned as 3-*O*-salicyloyl-5-*O*-benzoyl quinic acid (**10**) and 4-*O*-salicyloyl-5-*O*-benzoyl quinic acid (**11**).

Hemolymph Analysis Hemolymph samples of 6 *C. vinula* larvae were analyzed by UHPLC-ESI-MS/MS. Mass spectra were scanned for the presence of the molecular ions of compounds **1**–**11** (*m/z* 311, 295, 431, 415 ± 0.5 $[M-H]^-$) as well as for the molecular ions of salicortin (**12**, *m/z* 424 ± 0.5 $[M-H]^-$) and salicin (*m/z* 285 ± 0.5 $[M-H]^-$). None of these compounds were detected. Data are provided in Supplementary data (SI D.1 and D.2).

^{13}C-Labeling Study In order to investigate a possible precursor-product relationship of salicortin with the metabolites **1**–**11**, leaves of *P. nigra* were spotted with [U-^{13}C]salicortin (82% ^{13}C), as described in the Methods and Materials section (2.5), and subsequently fed to *C. vinula* larvae. The frass of larvae were extracted and analyzed by NMR and UHPLC-HRMS (see Supplementary data, C.2 and C.3). All larvae survived the feeding experiment without exhibiting negative effects arising from an elevated salicortin intake.

The ^{13}C NMR spectrum of the frass extract from the [U-^{13}C]salicortin feeding experiment showed signals characteristic for compounds **1**–**11**. Pronounced ^{13}C satellites appeared for signals of salicylates around δ_C 170, δ_C 165 and δ_C 135–130. No ^{13}C enrichment was found for glucosyl or quinate moieties (SI C.2–1 to C.2–5). Further structure elucidation was accomplished by 2D ^{1}H-^{13}C correlation spectroscopy. ^{1}H-^{13}C HSQC allowed for the identification of protons attached to the ^{13}C-enriched positions. The associated spin systems were assigned by selective TOCSY experiments to δ_H 7.93 (dd, $^3J_{HH}$ = 1.8/8.0 Hz)/δ_C 131.0, δ_H 7.98 (dd, $^3J_{HH}$ = 1.9/8.0 Hz)/δ_C 131.7 and δ_H 8.04 ($^3J_{HH}$ = 1.8/8.0 Hz)/δ_C 131.3, corresponding to salicylic acid moieties such as those observed for compounds **1**–**3** and **6**–**11**. The ^{1}H-^{13}C HMBC spectrum showed correlations of the salicylic acid moiety protons at δ_H 7.93 (δ_C 131.0; C-6), δ_H 7.98 (δ_C 131.6; C-6) and δ_H 8.04 (δ_C 131.3; C-6), with carbon atoms resonating at δ_C 136.7/136.5/136.2 (C-4), δ_C 162.1/162.8 (C-2) and δ_C 171.0/171.2/171.5 (C-7; COOH). ^{13}C-^{13}C Satellite signals for all those carbon signals indicated multiple ^{13}C enrichment of the salicyloyl moieties.

No ^{13}C-^{13}C satellites were observed in the ^{13}C NMR spectra and thus no ^{13}C enrichment occurred in the benzoyl units. The low intensity of the ^{1}H-^{13}C HMBC correlations of the benzoyl protons at δ_H 8.09 (δ_C 130.5; C-2/6) and δ_H 8.13 (δ_C 130.6; C-2/6) with δ_C 134.0 (C-4) and δ_C 168.1 (C-7; COOH) (Fig. 3 and SI C.2–6 to C.2–17) confirmed that the benzoyl units remained unlabeled.

Furthermore, UHPLC-HRMS spectra of the frass extract of *C. vinula* larvae fed with [U-^{13}C]salicortin showed ^{13}C-isotopologue patterns from $[M-H+3]^-$ up to $[M-H+7]^-$ (Fig. 4; C.3–1 to C.3–23). Remarkably, only salicylate-containing quinate esters, mono-salicyloyl quinates **1**–**3**, di-salicyloyl quinates **6**–**8** and salicyloyl-benzoyl quinates **9**–**11**, were labeled, and benzoyl quinates **4** and **5** showed no ^{13}C enrichment. The incorporation of ^{13}C from [U-^{13}C]salicortin into the salicyloyl moiety of the acylated quinic acids **1**–**3** and **6**–**11** clearly indicated a substrate-product relationship. Accordingly, we concluded that the acylated quinic acids were downstream products of the salicortin metabolism in *C. vinula*.

Another 7 (up to $[M-H+14]^-$) isotopologue peaks are present in the spectra of di-salicyloyl quinates **6**–**8**. The $[M-H+8]^-$ peak may be due to the presence of a natural abundance $^{13}C_1$ quinate or a $^{13}C_1$ salicyloyl substituent, in addition to the $^{13}C_7$-labeled first salicyloyl unit.

Discussion

The chemical defense of poplar includes abundant phenolic glycosides, such as salicortin and tremulacin, which can make up to 4% of the leaf dry mass (Boeckler et al. 2011; Donaldson et al. 2006). It is widely accepted that the digestive activation of salicinoids leads to toxic products warding off non-adapted herbivores. For salicortin, it has been proposed that activation proceeds through deglucosylation by β-glucosidases (Clausen et al. 1990; Lindroth 1988; Pentzold et al. 2014). The aglycon is either hydrolyzed spontaneously in the alkaline gut environment or degraded enzymatically by insect esterases (Lindroth et al. 1988; Lindroth 1989) to saligenin and a 1-hydroxy-6-oxocyclohex-2-en-1-oyl (HCH) fragment (Haruta et al. 2001; Julkunen-Tiitto and Meier 1992). The latter is believed to be oxidized to pyrocatechol and finally to *o*-quinone (Appel 1993; Barbehenn et al. 2010; Knuth et al. 2011; Ruuhola et al. 2003). *o*-Quinones have a high potential to bind to a variety of biomolecules, including amino acids and proteins (Haruta et al. 2001; Smith 1985). Generalist lepidopteran

species, such as the gypsy moth (*L. dispar*), have developed a strategy of detoxification (Boeckler et al. 2016) where the major salicinoids in *P. nigra*, salicortin and tremulacin, are transformed into typical metabolic phase II conjugates (Grant 1991), with salicin as the major metabolite (Boeckler et al. 2016).

The compounds **1**–**11** described in the present work are new quinic acid derivatives, isolated from the frass of *C. vinula*. The quinic acid moiety is substituted with either 1 or 2 salicylate units (**1**–**3**, **6**–**8**), benzoate units (**4**, **5**) or one of each unit (**9**–**11**). Compound **4** is the only compound that has been previously reported, namely as a constituent of fruits of *Ficus hirta* (Wan 2016). The results show that conjugation with quinic acid plays a decisive role in the transformation of salicinoids by *C. vinula*. The conjugation with quinic acids is described here for the first time as part of a detoxification pathway. Quinic acid has been reported to play a role in response to herbivory (Wang et al. 2016), and quinic acids were detected in the gut of insects (Crecelius et al. 2017). It was also suggested that quinic acid conjugates like chlorogenic acid produce feeding-deterrent compounds after cleavage and oxidative transformation of the phenylpropanoic part (Stevenson et al. 1993). The latter aspect needs to be clarified in the present example, and experiments addressing the question are ongoing.

Unlike in *L. dispar*, deglycosylation is an important feature of the metabolism in *C. vinula*, as glycosidic compounds or free sugars are absent in the frass extract. Generally, the salicinoid breakdown follows reported routes like deglucosylation, ester cleavage and conjugation (Clausen et al. 1990; Lindroth 1988; Pentzold et al. 2014). The structural diversity of the compounds – namely, the differential substitution of quinic acid with salicylate or benzoate – can be rationalized by acyl migration under basic conditions as present in the insect gut (Appel and Martin 1990). An enzymatic and hence stereospecific conjugation with quinic acid may take place at first, but those products rapidly isomerize later on. Another metabolite present after salicinoid degradation in *L. dispar*, hippuric acid, was absent in the [^{13}C]-metabolite spectrum of *C. vinula*. We can therefore conclude that hippuric acid is not a degradation product of salicortin, but arises likely from benzoyl-substituted structures like tremulacin.

The question of whether the source of salicyloyl units in quinic acid derivatives **1**–**11** were indeed salicinoid glycosides was tackled by stable isotope labeling experiments. *C. vinula* larvae were allowed to feed on leaves of *P. nigra* spotted with [U-^{13}C]salicortin (82% ^{13}C). Frass extracts were analyzed by means of NMR and HRMS. The resulting data were screened for isotopic incorporation into **1**–**11**. The isotopologue pattern of both NMR and HRMS spectra indicated differences in the incorporation of labeled salicortin into mono-salicyloyl quinic acids (**1**–**3**), mono-benzoyl quinic acids (**4**, **5**), bis-salicyloyl quinic acids (**6**–**8**) and salicyloyl-benzoyl quinic acids (**9**–**11**). NMR data showed enrichment of ^{13}C only in the salicyloyl moiety of quinic acid derivatives (Fig. 3). ^{13}C enrichment was further supported by HRMS data (Fig. 4) which showed a specific isotopologue pattern spanning from $[M-H]^-$ to $[M-H+7]^-$ for **1**–**3**. The HRMS spectra of **4** and **5** did not show additional ^{13}C-isotopologue signals. Thus, neither quinic acid nor benzoyl moieties is thought to represent a downstream product of the [U-^{13}C]salicortin precursor. This suggestion was further reflected in the HRMS data of **6**–**11**. Whereas mixed salicyloyl-benzoyl

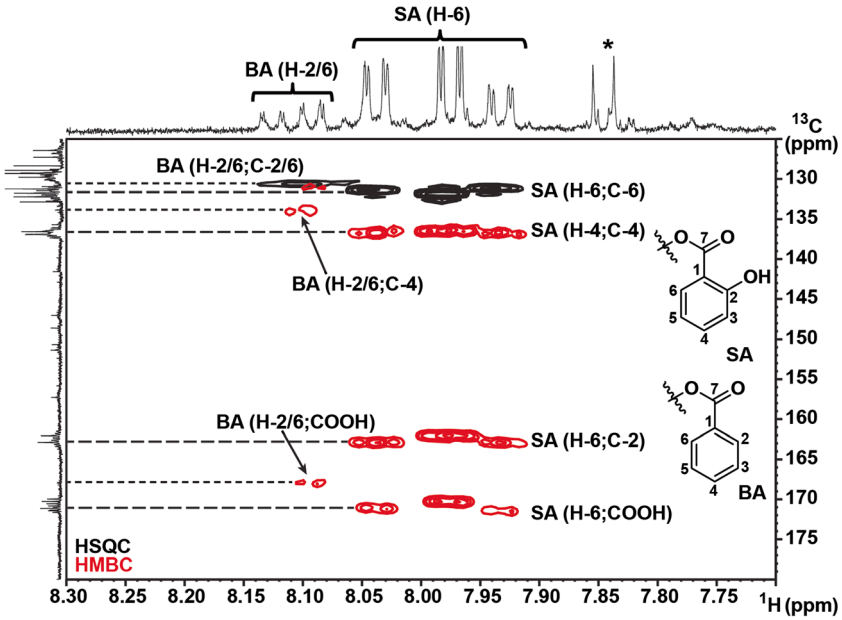

Fig. 3 Superimposed ^{1}H-^{13}C HSQC (black) and HMBC spectra (red) (500 MHz, MeOH-d_4) of *C. vinula* frass extract demonstrating ^{13}C enrichment of salicyloyl (SA) units but not of benzoyl (BA) units from [U-^{13}C]salicortin feeding. Top: Partial ^{1}H NMR spectrum showing signals of BA and SA. In the ^{13}C NMR spectrum (125 MHz) on the left, resonances of salicyloyl substituents show coupling patterns indicative of ^{13}C-enrichment. Cross-signals of * are not shown

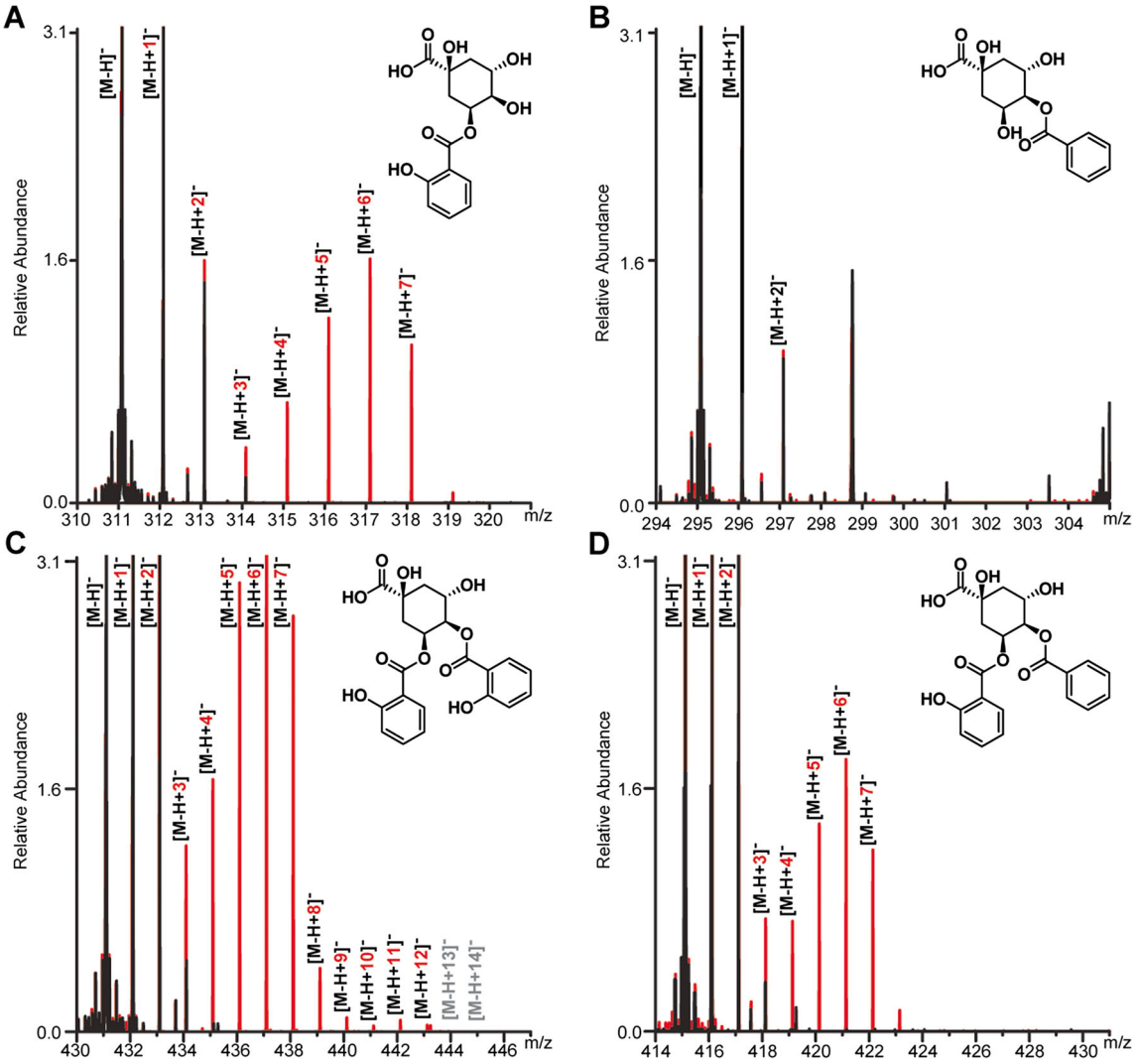

Fig. 4 Superimposed extracted ion HRMS spectra of the 4 acylated quinic acid groups – mono-salicyloyl quinates, mono-benzoyl quinates, di-salicyloyl quinates and salicyloyl-benzoyl quinates – isolated from the frass of *C. vinula* larva reared on [U-^{13}C]salicortin-coated *P. nigra* leaves (red) and unlabeled leaves (black). The groups are represented by compounds **1** (**A**), **4** (**B**), **6** (**C**) and **9** (**D**). The gray labeled isotopologue signals in panel **C** are very weak and thus not visible in this magnification

substituted compounds show only isotopologue signals up to $[M\text{-}H + 7]^-$, the bis-salicyloyl derivatives show signals up to $[M\text{-}H + 14]^-$.

Accordingly, this finding is a clear evidence that saligenin is transformed into salicylic acid. We assume that structurally similar salicinoids are transformed in an analogous manner. No ^{13}C incorporation was detected in the quinic acid moieties of **1**–**11**. Therefore, quinic acids likely originate from chlorogenic acids (caffeoyl quinates), which have already been described as leaf constituents of the Salicaceae (Caseys et al. 2015; Glynn et al. 2004). Considering the metabolic scheme in Fig. 5, it is important to note that there seems to be only one specific oxidative transformation of saligenin into salicylic acid in *C. vinula*. Likely, this specificity prevents the caffeoyl moiety of chlorogenic acid to be transformed into a toxic species (Felton et al. 1989) and facilitates quinic acids to scavenge the phenolic degradation products.

In our search for break-down products related to the HCH-moiety of salicortin, we did not find any further ^{13}C-labeled compound. Therefore, we speculate that there is a mechanism by which HCH degradation yields salicylic acid (Fig. 5). Under basic conditions, the HCH fragment could rearrange to an HCH-enolate followed by a spontaneous dehydration to form salicylic acid. The feasibility of such a transformation was observed in synthetic studies (Nagasawa et al. 2010). The origin of benzoyl substituents in **4**, **5**, **9**, **10** and **11** are likely common Salicaceae leaf constituents, such as chaenomeloidin, nigracin, populin, salireposid, tremulacin or tremuloidin (Boeckler et al. 2011).

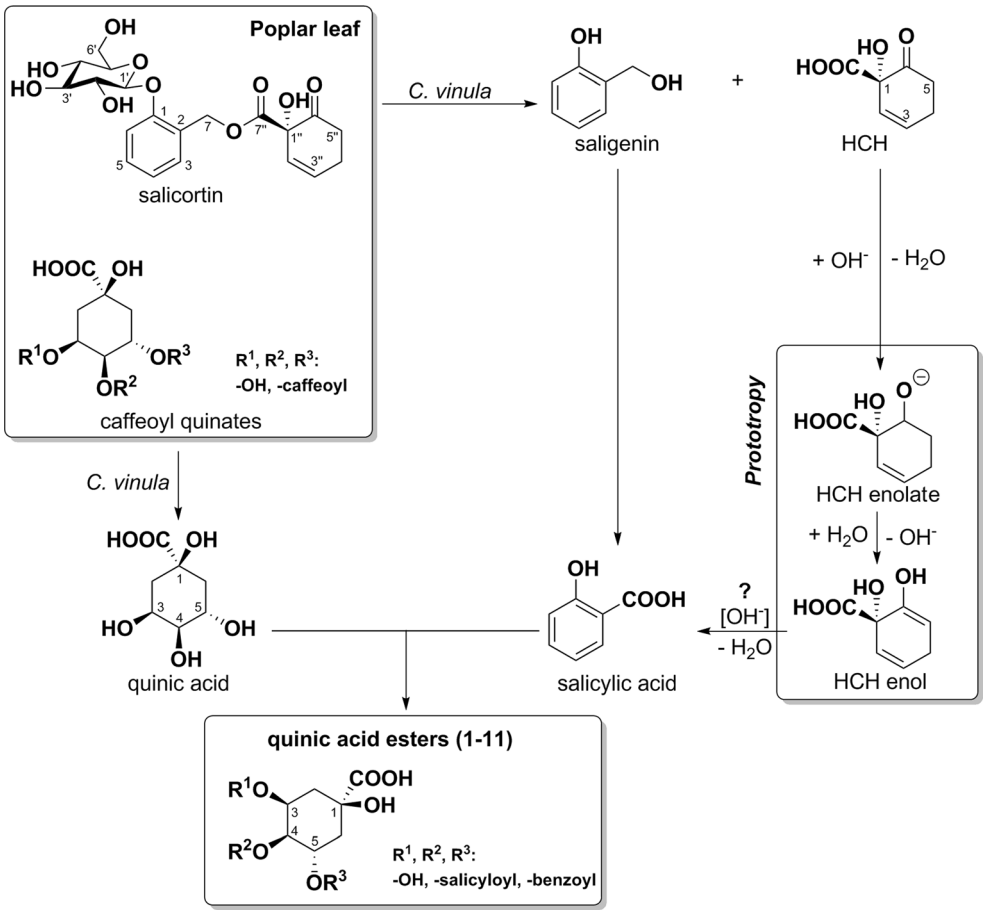

Fig. 5 Conversion of *Populus* leaf constituents to acylated quinic acid derivatives in the *C. vinula* larval gut

Acknowledgements Open access funding provided by Max Planck Society. The authors thank the workshop and IT-teams of the Max Planck Institute for Chemical Ecology for constructive cooperation, the greenhouse team for rearing the *Populus beaupré* trees, Regina Seibt for establishing the *C. vinula* breeding at our institute and Emily Wheeler for polishing the language.

References

Ali JG, Agrawal AA (2012) Specialist versus generalist insect herbivores and plant defense. Trends Plant Sci 17:293–302

Appel HM (1993) Phenolics in ecological interactions: the importance of oxidation. J Chem Ecol 19:1521–1552

Appel HM, Martin MM (1990) Gut redox conditions in herbivorous lepidopteran larvae. J Chem Ecol 16:3277–3290

Barbehenn R, Dukatz C, Holt C, Reese A, Martiskainen O, Salminen J-P, Yip L, Tran L, Constabel CP (2010) Feeding on poplar leaves by caterpillars potentiates foliar peroxidase action in their guts and increases plant resistance. Oecologia 164:993–1004

Beran F, Pauchet Y, Kunert G, Reichelt M, Wielsch N, Vogel H, Reinecke A, Svatoš A, Mewis I, Schmid D, Ramasamy S, Ulrichs C, Hansson BS, Gershenzon J, Heckel DG (2014) *Phyllotreta striolata* flea beetles utilize host plant defense compounds to create their own glucosinolate-myrosinase system. Proc Natl Acad Sci U S A 111:7349–7354

Boeckler GA, Gershenzon J, Unsicker SB (2011) Phenolic glycosides of the salicaceae and their role as anti-herbivore defenses. Phytochemistry 72:1497–1509

Boeckler GA, Paetz C, Feibicke P, Gershenzon J, Unsicker SB (2016) Metabolism of poplar salicinoids by the generalist herbivore *Lymantria dispar* (Lepidoptera). Insect Biochem Mol Biol 78:39–49

Burse A, Frick S, Discher S, Tolzin-Banasch K, Kirsch R, Strauß A, Kunert M, Boland W (2009) Always being well prepared for defense: the production of deterrents by juvenile *Chrysomelina* beetles (Chrysomelidae). Phytochemistry 70:1899–1909

Caseys C, Stritt C, Glauser G, Blanchard T, Lexer C (2015) Effects of hybridization and evolutionary constraints on secondary metabolites: the genetic architecture of phenylpropanoids in European *Populus* species. PLoS One 10:23

Chen W-P, Yang X-Y, Harms GL, Gray WM, Hegeman AD, Cohen JD (2011) An automated growth enclosure for metabolic labeling of *Arabidopsis thaliana* with ^{13}C-carbon dioxide - an *in vivo* labeling system for proteomics and metabolomics research. Proteome Sci 9:9

Clausen TP, Reichardt PB, Bryant JP, Werner RA, Post K, Frisby K (1989) Chemical model for short-term induction in quaking aspen (*Populus tremuloides*) foliage against herbivores. J Chem Ecol 15:2335–2346

Clausen TP, Koller JW, Reichardt PB (1990) Aglycone fragmentation accompanies β-glucosidase catalyzed hydrolysis of salicortin, a

naturally-occurring phenol glycoside. Tetrahedron Lett 31:4537–4538

Crecelius AC, Michalzik B, Potthast K, Meyer S, Schubert US (2017) Tracing the fate and transport of secondary plant metabolites in a laboratory mesocosm experiment by employing mass spectrometric imaging. Anal Bioanal Chem 409:3807–3820

Donaldson JR, Stevens MT, Barnhill HR, Lindroth RL (2006) Age-related shifts in leaf chemistry of clonal aspen (*Populus tremuloides*). J Chem Ecol 32:1415–1429

Feistel F, Paetz C, Lorenz S, Schneider B (2015) The absolute configuration of salicortin, HCH-salicortin and tremulacin from *Populus trichocarpa x deltoides* Beaupré. Molecules 20:5566–5573

Felton GW, Donato K, Del Vecchio RJ, Duffey SS (1989) Activation of plant foliar oxidases by insect feeding reduces nutritive quality of foliage for noctuid herbivores. J Chem Ecol 15:2667–2694

Glynn C, Ronnberg-Wastljung AC, Julkunen-Tiitto R, Weih M (2004) Willow genotype, but not drought treatment, affects foliar phenolic concentrations and leaf-beetle resistance. Entomol Exp Appl 113:1–14

Grant DM (1991) Detoxification pathways in the liver. J Inherited Metab Dis 14:421–430

Haruta M, Pedersen JA, Constabel CP (2001) Polyphenol oxidase and herbivore defense in trembling aspen (*Populus tremuloides*): cDNA cloning, expression, and potential substrates. Physiol Plant 112: 552–558

Hintze-Podufal C (1970) Über die quantitativen Änderungen der Kotabgabe während der Larvalentwicklung von *Cerura vinula* L. (Lepidoptera). Oecologia 5:334–346

Joussen N, Agnolet S, Lorenz S, Schone SE, Ellinger R, Schneider B, Heckel DG (2012) Resistance of Australian *Helicoverpa armigera* to fenvalerate is due to the chimeric P450 enzyme CYP337B3. Proc Natl Acad Sci USA 109:15206–15211

Julkunen-Tiitto R, Meier B (1992) The enzymatic decomposition of salicin and its derivatives obtained from salicaceae species. J Nat Prod 55(9):1204–1212

Knuth S, Schübel H, Hellemann M, Jürgenliemk G (2011) Catechol, a bioactive degradation product of salicortin, reduces TNF-α induced ICAM-1 expression in human endothelial cells. Planta Med 77: 1024–1026

Lindroth RL (1988) Hydrolysis of phenolic glycosides by midgut β-glucosidases in *Papilio glaucus* subspecies. Insect Biochem 18: 789–792

Lindroth RL (1989) Biochemical detoxication: mechanism of differential tiger swallowtail tolerance to phenolic glycosides. Oecologia 81: 219–224

Lindroth RL (1991) Biochemical ecology of aspen-Lepidoptera interactions. J Kans Entomol Soc 64:372–380

Lindroth RL, Hemming JDC (1990) Responses of the gypsy moth (Lepidoptera: Lymantriidae) to tremulacin, an aspen phenolic glycoside. Environ Entomol 19:842–847

Lindroth RL, Scriber JM, Hsia MTS (1988) Chemical ecology of the Tiger swallowtail - mediation of host use by phenolic glycosides. Ecology 69:814–822

Nagasawa T, Shimada N, Torihata M, Kuwahara S (2010) Enantioselective total synthesis of idesolide via $NaHCO_3$-promoted dimerization. Tetrahedron 66:4965–4969

Palo RT (1984) Distribution of birch (*Betula* spp.), willow (*Salix* spp.), and poplar (*Populus* spp.) secondary metabolites and their potential role as chemical defense against herbivores. J Chem Ecol 10:499–520

Pauli GF, Poetsch F, Nahrstedt A (1998) Structure assignment of natural quinic acid derivatives using proton nuclear magnetic resonance techniques. Phytochem Anal 9:177–185

Pentzold S, Zagrobelny M, Rook F, Bak S (2014) How insects overcome two-component plant chemical defence: plant β-glucosidases as the main target for herbivore adaptation. Biol Rev Cambridge Philos Soc 89:531–551

Ruuhola T, Tikkanen O-P, Tahvanainen J (2001) Differences in host use efficiency of larvae of a generalist moth, *Operophtera brumata* on three chemically divergent *Salix* species. J Chem Ecol 27:1595–1615

Ruuhola T, Julkunen-Tiitto R, Vainiotalo P (2003) *In vitro* degradation of willow salicylates. J Chem Ecol 29:1083–1097

Shelomi M, Heckel DG, Pauchet Y (2016) Ancestral gene duplication enabled the evolution of multifunctional cellulases in stick insects (Phasmatodea). Insect Biochem Mol Biol 71:1–11

Smith MT (1985) Quinones as mutagens, carcinogens, and anticancer agents: introduction and overview. J Toxicol Environ Health 16: 665–672

Stevenson PC, Anderson JC, Blaney WM, Simmonds MS (1993) Developmental inhibition of *Spodoptera litura* (fab.) larvae by a novel caffeoylquinic acid from the wild groundnut, *Arachis paraguariensis* (Chod et Hassl.) J Chem Ecol 19:2917–2933

Thieme H (1964) Isolierung eines neuen Phenolglucosids aus *Salix purpurea* L. Pharmazie 19:725

Wan C, Han J, Chen C, Yao L, Chen J, Yuan T (2016) Monosubstituted benzene derivatives from fruits of *Ficus hirta* and their antifungal activity against phytopathogen *Penicillium italicum*. J Agric Food Chem 64:5621–5624

Wang L, Qu L, Zhang L, Hu J, Tang F, Lu M (2016) Metabolic responses of poplar to *Apripona germari* (hope) as revealed by metabolite profiling. Int J Mol Sci 17:923